AIAA AVIATION Forum
June 27-July 1, 2022, Chicago, IL & Virtual
AIAA AVIATION 2022 Forum
10.2514/6.2022-3289

Bypass Ratio Parametric Analyses on a Narrow-Body Aircraft Using a New Tool for Turbofan Rubberization

M. Di Stasio[1], V. Trifari[2], F. Nicolosi[3] and A. De Marco[4]
University of Naples Federico II, Naples, 80125, Italy

R. Schaber[5]
MTU Aero Engines AG, Munich, 80995, Germany

A major issue which has usually prevented aircraft manufacturers from implementing efficient and cost-effective design processes is the loose integration of engine models into iterative aircraft design workflows. This work aims at reducing this gap, by introducing a simplified modeling of the behavior of a gas turbine, allowing to rubberize a generic turbofan engine. In the present context, this methodology has been implemented for a two-spool, direct-drive, unmixed flow turbofan, but it could be easily extended to different engine configurations (e.g., geared turbofan). In order to prove the effectiveness of this approach, this rubber engine model has been included in an already existing aircraft design framework and has been used to carry out parametric analyses on engine bypass ratio, aiming at guiding the selection of this engine parameter for an advanced short-haul narrow-body aircraft.

I. Nomenclature

A/C	=	aircraft
API	=	application programming interface
ARC	=	aerodrome reference code
BRF	=	body reference frame
BPR	=	bypass ratio
CAS	=	calibrated air speed
CFRP	=	carbon-fiber-reinforced polymers
ECS	=	environmental control system
EI	=	emission index
EIS	=	entry into service
EoR	=	end of runway
FCS	=	flight control system
HBPR	=	high bypass ratio
HPC	=	high-pressure compressor
HPT	=	high-pressure turbine
IPS	=	ice protection system
ISA	=	international standard atmosphere
LE	=	leading edge
LFL	=	landing field length
LG	=	landing gears
LPC	=	low-pressure compressor
LPT	=	low-pressure turbine
MAC	=	mean aerodynamic chord
MDA	=	multi-disciplinary analysis
MEA	=	more-electric aircraft
MTOW	=	maximum take-off weight
OBS	=	on-board systems
OEW	=	operating empty weight
OPR	=	overall pressure ratio
ROC	=	rate of climb
ROD	=	rate of descent
SLS	=	sea-level static
sNO_x	=	NO_x severity index
SPL	=	sound pressure level
T_3	=	HPC exit temperature
T_4	=	burner exit temperature
T_{45}	=	LPT entry temperature
T/O	=	take-off
T/W	=	thrust-to-weight ratio
TLAR	=	top-level aircraft requirement
ToC	=	top of climb
TOFL	=	take-off field length
TSFC	=	thrust-specific fuel consumption
W/S	=	wing loading

[1] PhD Student, Dept. of Industrial Engineering, mario.distasio@unina.it
[2] Post-doctoral Researcher, Dept. of Industrial Engineering, vittorio.trifari@unina.it
[3] Full Professor, Dept. of Industrial Engineering, fabrizio.nicolosi@unina.it, AIAA Member
[4] Associate Professor, Dept. of Industrial Engineering, agostino.demarco@unina.it
[5] Consultant Predesign Methodology, Engineering Advanced Programs, reinhold.schaber@mtu.de

II. Introduction

Modern civil transport aircraft involve several subsystems which are designed, in general, to have the lowest possible weight and the highest possible efficiency, so as to minimize their impact on the overall aircraft performance. This same criterium applies to the powerplant system of a modern aircraft, which needs to be specifically designed and built, to meet all the necessary requirements and constraints in terms of performance (thrust and fuel consumption), emissions, noise and costs. Actually, an effective integration between the design of the aircraft and that of the engines is something which has started to be radically implemented only in recent years. Traditionally, the design of a new aircraft has always been decoupled from the engine design. Even for supersonic military applications, for which the matching between the two designs represents a crucial aspect, an integrated approach supported by dedicated tools has started to be adopted only from the 1990s. For civil transport aircraft, this radical change in the overall design process has been effectively put into practice only for the latest development programs, such as the ones for the Boeing 787 or the Bombardier C Series (now Airbus A220), during which the engine manufacturers, Rolls-Royce/GE and Pratt & Whitney respectively, were involved in the overall design process of the aircraft since the earliest stages.

In order to enable this radical change, aircraft designers should be supported by dedicated tools, allowing to easily and promptly perform, at conceptual design stage, trade-off studies involving information related to the behavior of the powerplant system in terms of performance, emissions, dry mass, main dimensions, environmental noise, and costs, by linking these changes to key engine design parameters, such as the Bypass Ratio (BPR), the Overall Pressure Ratio (OPR) and the burner exit temperature (T_4). This type of approach, from one side, would allow aircraft designers to have, even from early conceptual design stages, more precise figures on the powerplant, noticeably increasing the number and the quality of information available on the aircraft-engine integration process. On the other side, aircraft designers would be allowed to provide important indications to engine designers on which set of design input variables should grant the matching of aircraft requirements, while trying to optimize mission fuel burn, emissions, noise, and costs.

The creation of a tool with these characteristics, supporting aircraft preliminary design phases, was one of the main objectives of the collaboration between the University of Naples Federico II (UNINA) and MTU Aero Engines for a three-month internship (performed in smart working, due to the COVID pandemic) involving one UNINA PhD student and engine design experts from MTU. The present work has been carried out within the context of the Clean Sky 2 project ADORNO [1]. This project includes, among its high-level objectives, the integration of engine-related aspects and effects in the preliminary design process of a novel aircraft configuration, in order to drastically reduce the necessary design time to converge for aircraft and engine design loops. However, the work and the results reported in this paper do not represent the outcomes of ADORNO, and they are just the consequence of the collateral collaboration between the partners in the project.

III. Objective of the work

The main objective of this paper is to provide an overview on the methodology and the tools that were elaborated in order to generate a rubber engine model that could be easily integrated in an aircraft design framework. This description has been included in Section IV, along with a brief explanation on its integration in an existing aircraft design and analysis tool.

Such a rubber turbofan engine model was used to guide the choice on the best suitable BPR, leading to the lowest possible mission block fuel, for a High-Bypass Ratio (HBPR), direct-drive, two-spool engine, to be equipped on an advanced short-haul, narrow-body aircraft, with an expected Entry Into Service (EIS) in 2030. This advanced aircraft model was equipped with advanced airframe technologies, such as More-Electric Aircraft (MEA) architecture allowing for a bleedless (i.e., zero overboard bleed) engine configuration. The results of these analyses have been reported in Section V. This section also provides information on how the baseline aircraft configuration used for these studies was generated, as well as details on the assumptions that were performed regarding the impact of advanced airframe technologies on aircraft weights, aerodynamics, and power off-takes.

IV. Rubber engine model generation and implementation

This tool for a simplified preliminary engine design was developed for a specific engine architecture (direct-drive, two-spool, unmixed flow turbofan) and was successfully included in an existing tool for preliminary aircraft design, namely JPAD [2][3]. The JPAD structure of sub-modules serving Multi-Disciplinary Analyses (MDA) workflows did already include a static description of the characteristics of the powerplant, with information coming from the engine being used to estimate the design weights of the aircraft, the aerodynamics, the performance, the emissions, the environmental noise at certification points, and the costs. Since these were considered frozen information about the engine, they could not be dynamically updated during an MDA workflow. Or they could be eventually updated, such as for the Sea-Level Static (SLS) thrust, the overall dimensions of the engine/nacelle and the dry mass, but modifications were mainly performed based on statistical assumptions rather than a knowledge-based approach. With the support of a preliminary engine design tool instead, the paradigm reported in Fig. 1 could be actually enabled and provide much more reliable results.

The generation of this rubber engine model went through different phases and different supporting calculation tools, which have been summarized in Fig. 2. The approach reported in this figure is a particularization to the turbofan case of the methodology elaborated in Ref. [4], which, as it was proved, can be applied to quite different engine architectures for aeronautical applications.

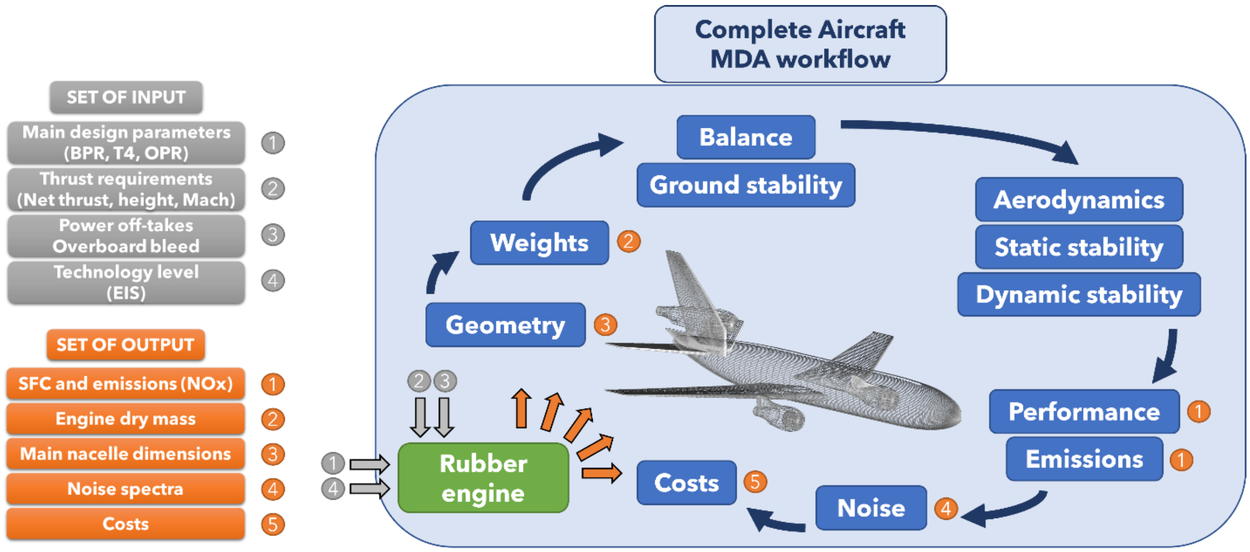

Fig. 1 Inclusion of an engine preliminary design tool in a typical aircraft MDAO work chain.

A. Rubber model implementation in an engine performance tool

The first phase required the selection of a reference architecture and thrust class, in order to guide some of the assumptions regarding the set of input design variables of the engine. As already mentioned before, the selected reference was for a direct-drive, two-spool, unmixed flow turbofan, with the same general architecture of the LEAP-1A model produced by CFM International, which represents the current state-of-the-art for this engine category.

The next step consisted in the implementation of a reliable representation of the behavior of this engine, both at design and off-design conditions, in a gas turbine performance calculation tool. GasTurb [5] (version 11) was used for this task, since it allows to easily perform both the operations, supporting off-design simulations in particular by means of default maps for compressors and turbines, which can be adequately and automatically scaled depending on the specific application.

The GasTurb template engine model for a geared, unmixed flow, turbofan engine, which can be easily converted to the one for a direct-drive engine by selecting a value of the gear ratio equal to 1.0, was selected as the starting point for the construction of a rubber engine model. To ensure the consistency and the reliability of the results produced by this model, several design laws and criteria for automatic cycle updates were introduced, by taking advantage of all the supporting features and modules (i.e., definition of additional input parameters and composed values, definition of look-up tables, iterative mode) provided by GasTurb. This approach mainly followed (and simplified, at least for certain aspects) the example of Ref. [6]. Top of Climb (ToC) was selected as the design point condition for the engine, in order to consistently set the fan diameter (and the overall size of the engine in general). Automatic update laws were set at design point for the following variables of the engine:

- Setting of the entry mass flow rate by iterating over a target value for the net thrust at design point.
- Setting of the outer and inner fan pressure ratios, by using the ideal jet velocity ratio (i.e., the ratio between ideal fan and core exhaust velocities) as an iteration target, as suggested in Ref. [7].

- Determination of the pressure ratio split between the Low-Pressure Compressor (LPC), the High-Pressure Compressors (HPC) and the inner fan, starting from a provided OPR value (set as an additional input variable in the GasTurb model).
- Definition of the average circumferential speeds of the fan and of the HPC, starting from statistical data available in Ref. [8].
- Basic gas path modeling, starting from the definition of reference values for entry/exit hub-to-tip ratios and flow Mach numbers, both for compressors and turbines. These values were set once and for all, starting from available information and cutaway diagrams of the reference engine, and from reasonable indications derived from the literature on the topic [8][9][10].
- Estimation of the mean stage loading, according to the definition given in Ref. [8], of the HPC and the High-Pressure Turbine (HPT), starting from input values for the number of stages (which were deemed constant and equal to the ones of the reference engine). Estimation of the required number of stages of the LPC and the Low-Pressure Turbine (LPT), starting from fixed values of the mean stage loading, taken from statistical data available in Ref. [8]. These information could be later used to eventually discard unfeasible engine designs, featuring a too high number of stages, which for sure would lead to problems linked to their manufacturing complexity and weight.
- Determination of the amount of cooling air required by the HPT (the LPT was supposed uncooled, as the one of the reference engine), starting from the input in terms of required thrust at Take-Off End-of-Runway (T/O EoR) condition. For this purpose, a surrogate model for cooling air demand was preliminarily built, by performing off-design analyses to estimate cycle temperatures, which were then used to calculate the actual cooling air demand using the approach reported in Ref. [11]. Input variables of this model related to the technology level of the cooling system and to the maximum allowable temperature of the turbines materials were linked to an input variable of the rubber engine model accounting for the EIS.
- Estimation of the polytropic efficiency of each component by means of a model built starting from data and assumptions suggested in Ref. [8]. In this reference, normalized polytropic efficiency values of compressors and turbines are provided as a function of mean stage pressure ratio and/or average stage loading, through several plots based on actual engine data. These data are normalized with respect to engine size, Reynolds number, EIS, and, for the turbine case, cooling air demand. The same source also provides plots and equations to be used to transform, through the application of corrections, normalized data into actual efficiency data. The plots provided in Ref. [8] were used to determine a set of equations, similarly to what was done in Ref. [12], for the consistent estimation of the efficiencies of the turbo components of the engine. These equations were then directly implemented into GasTurb.
- Setting of the pressure losses at the inlet and along the compressors and turbines inter-ducts, according to the values suggested in Ref. [9].
- Calculation of nozzle thrust and discharge coefficients, according to the simplified modeling suggested in Ref. [6], relying on statistical data available in Ref. [8].
- Setting of the mechanical efficiencies of low-pressure and high-pressure spools according to reference values provided in Ref. [9].

Through the implementation of the above-listed set of assumptions and consistent relationships, a linkage was created, at design point, between the overall set of engine input variables and the following, limited, list:

- BPR,
- OPR,
- Burner exit temperature,
- Net thrust,
- Operating conditions (i.e., flight altitude and Mach number),
- Off-design (T/O EoR) net thrust,
- Power off-takes and overboard bleed,
- EIS.

The rubber engine model implemented in GasTurb was thoroughly tested against public available data of existing engines, also belonging to a different thrust class with respect to the reference one. These tests provided acceptable results in terms of Thrust-Specific Fuel Consumption (TSFC) prediction, with differences always in the range between 2 and 5%.

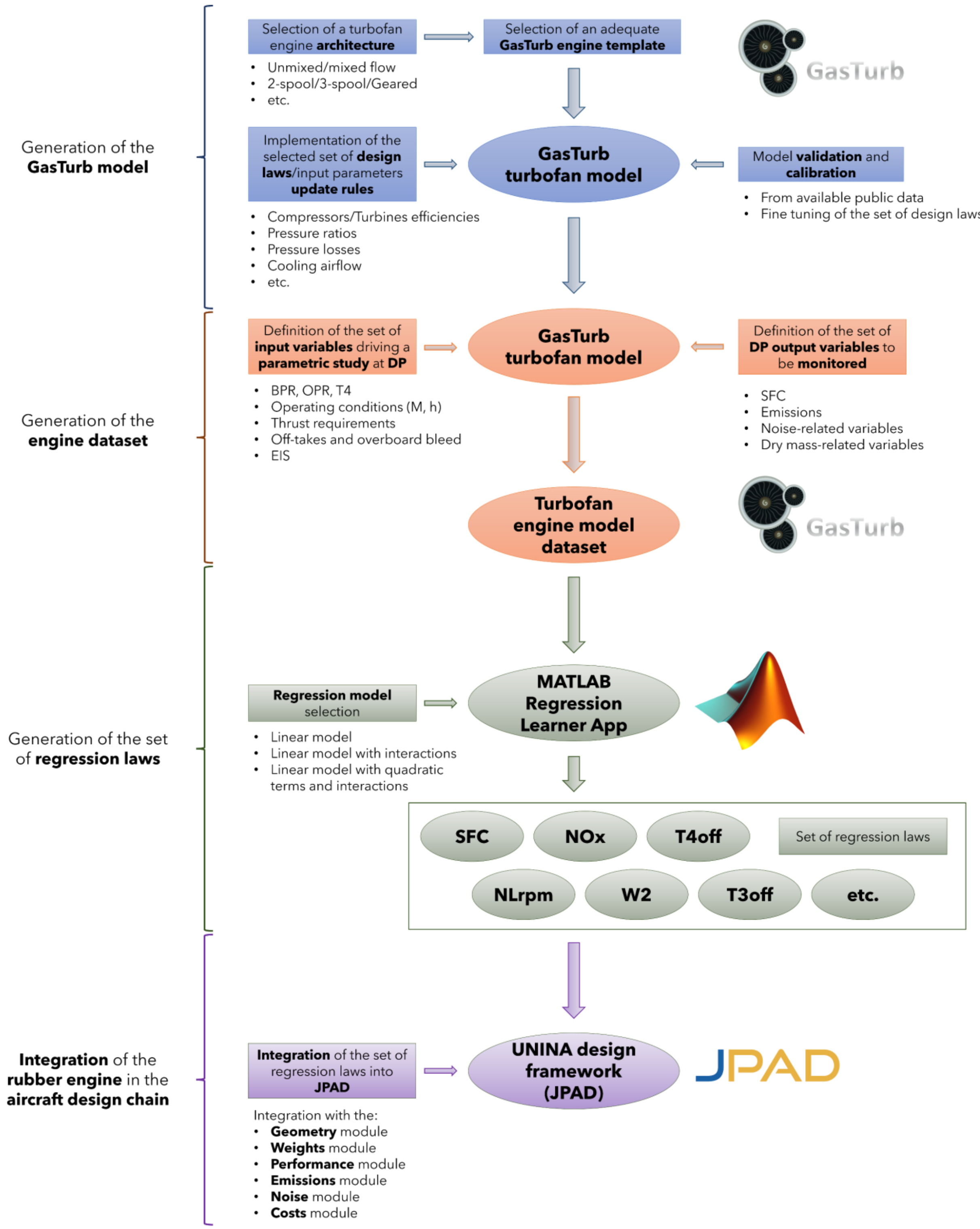

Fig. 2 Main steps for the generation of a rubber turbofan module to be included in the aircraft design workflow of JPAD.

B. Generation of the engine dataset

After performing calibration and validation of this model based on available public information, work was performed to generate a dataset, to be later used to create a surrogate rubber engine that could be easily implemented in a generic aircraft design framework. Parametric studies were performed in GasTurb, involving the set of input variables listed in the previous sub-section.

Several cycle output variables were tracked in these studies, in order to adequately model the behavior of the engine. In particular, the following information were included in the dataset:

- ToC TSFC, to scale data on fuel consumption (per engine rating and flight condition) included in a reference customer deck, which was produced starting from the design point of the LEAP-1A engine, generated by using the rubber turbofan model implemented in GasTurb.
- ToC NO_x severity index (sNO_x), in order to perform the same operation described above, but this time for the NO_x Emission Index (EI).
- Fan diameter, in order to adequately model the size of the engine, by using scale factors and equations derived from the literature in order to estimate the nacelle cowl length [13], the maximum nacelle diameter, and the nacelle cowl exit diameter.
- Fan temperature rise, fan entry mass flow rate, and fan tip Mach number, to perform a preliminary estimation of the noise produced by the engine, by adopting the methodology for fan/compressor noise described in Ref. [14].
- SLS T/O BPR, OPR, and core mass flow rate, to allow the estimation of the dry mass of the engine according to the methodology described in Ref. [15]. In order to allow the estimation of these cycle variables at design point, a surrogate model was previously generated, as with the cooling air demand, by carrying out several off-design calculations at SLS T/O conditions.
- T/O EoR HPC exit temperature, burner exit temperature, and LPT entry temperature, to eventually restrict the available design space for certain combinations of input design variables and discard unfeasible design solutions. Reasonable temperature limitations were linked to the EIS value of the model, by mainly using information and suggestions included in Refs. [16][17].
- Tip and circumferential speeds of all the turbomachineries, for the same reason expressed above, but this time for the need to consider mechanical limitations. Ref. [9] provided most of the values that were used to set these constraints. These values were double-checked by also considering indications provided in Ref. [8].
- LPC and LPT number of stages, to discard complicated solutions from a manufacturing point of view.

Adequate boundaries were selected for the input design variables of the parametric studies, in order to have the widest possible design space. BPR values ranged between 8 and 14, whereas the OPR and the T_4 where changed in the range between 45 and 60, and from 1550 to 1900 K, respectively. Data was produced for three specific EIS values, 2015, 2030 and 2040, in order to allow the final surrogate rubber engine to provide information both for current state-of-the-art engines and for evolutionary engine designs.

C. Generation of the set of regression laws

The dataset produced with these parametric studies was used to train a separate linear regression model for each of the cycle output variables of interest, in order to generate a surrogate model of the engine that could be effectively exported and implemented in an aircraft preliminary design and analysis tool, enabling to perform trade-off analyses and optimizations at airplane level.

The MATLAB Regression Learner App [18] was used for this purpose. This application provides several training models, even much more complicated than the linear one and that are more flexible to the provided dataset. The main advantage of linear models within this context consisted in their easy interpretability (i.e., simple linear formulas are used to perform data regression) and in the possibility to effortlessly export the trained models to applications outside the MATLAB environment. For the linear model there are several options provided by the application, allowing to eventually include an increasing number of terms in the model. It was tested that for the majority of the output variables of interest, only the quadratic model (i.e., a linear model including a constant term, linear terms, interaction terms and quadratic terms) would have granted reasonably low values of the root mean square errors, thus a good fitting of the regression model to the output data of GasTurb.

D. Integration in an aircraft design chain

The final step consisted in the integration of this surrogate engine model in the JPAD structure of calculation modules for the design, analysis and optimizations of civil aircraft. This was performed by including in the set of

JPAD sub-modules an additional calculator dedicated to preliminary engine design, including the set of previously generated regression laws, and providing output in terms of:

- Performance and emissions, by way of scaling factors for thrust, TSFC and sNOx to be applied to an existing reference engine deck, including data on these performance of the engine for different ratings (max. take-off, max. continuous, max. climb, cruise, flight and ground idle), different throttle settings, and different operating conditions (flight altitude, flight speed and ISA deviation).
- Dry mass, using the multi-equation and multi-parameter method of Ref. [15].
- Engine (fan diameter and overall length) and nacelle (maximum transversal dimension, cowl length, bypass duct exit diameter) size.
- Fan noise, in the form of Sound Pressure Level (SPL) spectra for different engine ratings and throttle settings, to be interpolated by the JPAD module for preliminary aircraft noise estimations [19].
- Costs-related estimations, using simple semi-empirical equations for development cost, development time and production costs provided in Ref. [20].

Fig. 3 provides an example of the data produced by the surrogate engine model in terms of TSFC, dry mass, fan diameter, and fan tip Mach number, for different combinations of design T_4 and BPR. Furthermore, an example of usage of the information on the T/O EoR engine temperatures has been provided in Fig. 4, highlighting how those information could be used to restrict the available design space. This contour plot could be also produced including the effect of mechanical and manufacturing limitations, as previously described.

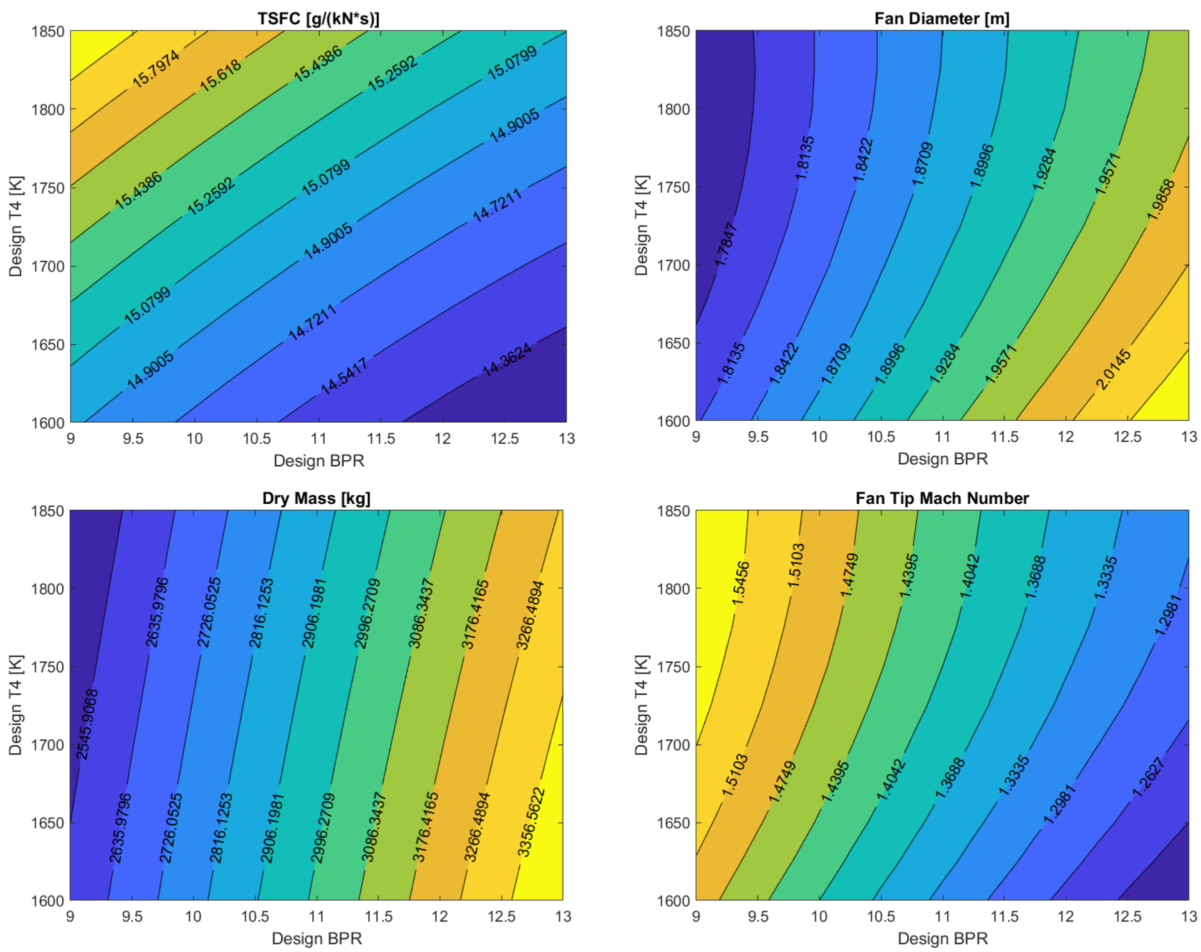

Fig. 3 Exemplificative output of the surrogate engine model in terms of contour plots for TSFC, dry mass, fan diameter, and fan tip Mach number, with respect to variation in terms of design burner exit temperature and design BPR. Remaining input parameters set according to data reported in Table 1.

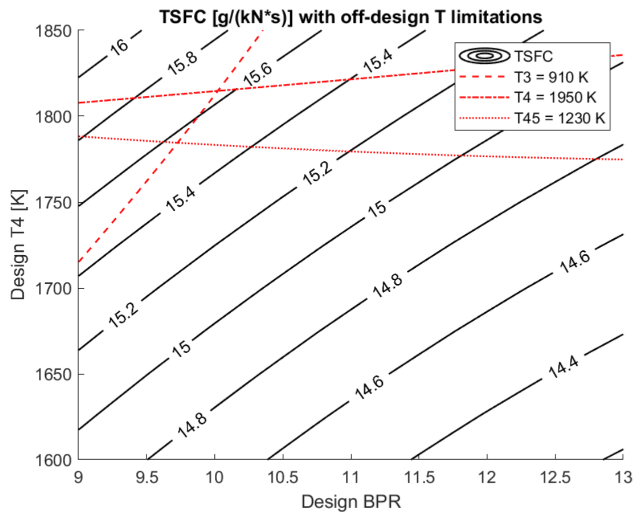

Fig. 4 Example of usage of the off-design temperatures (T_3 is the HPC exit temperature, T_4 is the burner exit temperature, and T_{45} is the LPT entry temperature at T/O EoR condition) in order to restrict the engine design space. Limiting temperature values in this case are purely illustrative. Remaining input parameters set according to data reported in Table 1.

Table 1. Remaining input parameters for the contour plots of Fig. 3 and Fig. 4.

Input parameter	Value		Input parameter	Value
EIS	2015		ToC net thrust	25 kN
OPR	45		T/O EoR net thrust	94 kN
Mach number	0.78		Overboard bleed	0.0 kg/s
Flight altitude	35000 ft		Power off-takes	0.0 kW

V. Rubber engine model application

The following sub-sections provide an example of application of the previously described surrogate model of a turbofan engine for a parametric analysis on BPR. This study helped to further check the capability of this model to provide physically plausible results, when coupled with the parametric aircraft models of JPAD.

A. Statistical generation of a baseline model

The JPAD module for Pre-Design activities (already described in Ref. [2]) was employed to generate a baseline aircraft for a parametric analysis on engines BPR. Top-Level Aircraft Requirements (TLAR) for a short-haul, narrow-body airliner, similar to the Airbus A320 or the Boeing B737, were used to generate a statistical aircraft. TLAR were provided to the tool in terms of mission requirements (e.g., number of passengers to be carried on board, design range, rate of climb, climb speed, cruise altitude, cruise Mach number, etc.), and aircraft configuration (e.g., wing position, tail configuration, engines type, engines position, etc.). These requirements have been summarized in Table 2.

Additional input information required by the Pre-Design module were automatically calculated, by means of the set of statistical equations and assumptions provided by the same tool. These automatic settings involved in particular:

- The estimation of the Oswald factor for the take-off, the cruise, the approach, and the landing phases, using the equations and the suggestions provided in Ref. [21].
- The calculation of the zero-lift coefficient of the aircraft by means of the flat-plate analogy.
- The calculation of the lift coefficients for the characteristic point on the parabolic drag polar, leading to a preliminary estimation of reasonable values of the lift coefficients for the cruise, the alternate cruise, and the holding phases.
- The determination of the drag polar curves of the aircraft for the main flight phases, using the well-known parabolic drag polar equation.

These basic information on a preliminary aerodynamics of the aircraft were used by the Pre-Design module to carry out the estimation of the aerodynamic efficiency of the airplane, to be used, along with assumptions on engine TSFC and fuel fraction weights, for a first estimation of the aircraft Maximum Take-Off Weight (MTOW) and of the Operating Empty Weight (OEW). The values for the TSFC per phase were automatically selected by the tool, thanks to its implemented set of statistical relationships. Fuel fractions for the cruise, the alternate, and the holding phases were calculated by the module using the classical Breguet equations. Whereas the fuel fractions for the remaining phases were also automatically assumed, on the basis of statistical data implemented by the module.

Sizing limitations were then calculated, concerning take-off field length, landing field length, cruise speed, and climb requirements. These limitations were used to select a feasible sizing point of the aircraft, according to a strategy to maximize the wing loading (W/S) of the airplane. After the definition of the sizing point, the SLS thrust and the wing planform area were determined, which could eventually differ from the values used for the original assumptions made for the aerodynamics and the fuel consumption of the aircraft. For this reason, a fully-automatic, iterative update of the sizing point (according to the same strategy reported above) was carried out by the tool, leading to a converged final solution, whose main characteristics have been summarized in Table 3, and for which a visual representation has been provided in Fig. 5. The final analysis of the baseline model, whose results have been included in Table 3, was carried out using the module of JPAD for MDA, involving a simulation-based approach for the calculation of the performances of the airplane [22], as well as a more detailed calculation of the aerodynamics and the weights. It is important to highlight also that the characteristics of the powerplant, with the exception of the BPR and the SLS T/O thrust, were determined for this detailed analysis through the turbofan surrogate model, assuming a 2015 EIS, an OPR equal to 50 and a T_4 of 1800 K, which should be close to the characteristics of the LEAP-1A.

Table 2 Set of TLAR adopted for the automatic, statistical generation of a baseline aircraft model.

Requirement	Value	Requirement	Value	Requirement	Value
Design passenger number	165	Cruise Mach number	0.78	Holding Mach number	0.55
Design range	3500 nmi	Cruise altitude	35000 ft	Holding altitude	1500 ft
TOFL	1950 m	Alternate Mach number	0.65	Holding duration	30 min
LFL	1650 m	Alternate altitude	20000 ft	Descent CAS	275 kn
Climb CAS	290 kn	Alternate range	200 nmi	Descent ROD	2250 ft/min
Climb ROC	2000 ft/min				

Table 3 Main characteristics of the baseline aircraft model, defined through the JPAD Pre-Design tool, and analyzed with the MDA module.

Geometry	Value	Design Weights	Value
Wing planform area	126.1 m	MTOW	78750 kg
Wing aspect ratio	10.16	OEW	43950 kg
Wing span	35.8 m	**Performance**	**Value**
Wing MAC	4.05 m	TOFL	1995 m
Wing sweep angle LE	28 deg	LFL	1610 m
Powerplant	**Value**	Block fuel	17650 kg
SLS T/O thrust	118 kN	Total fuel	19850 kg
BPR	11	Total CO_2	62500 kg
Max. nacelle diameter	2.58 m	Total NO_x	321 kg

Fig. 5 Render of the 3D model of the baseline aircraft, automatically generated with JPAD.

B. Parametric analyses on engine BPR

The aircraft model, generated through the JPAD Pre-Design module as described in the previous sub-section, was later used as the baseline for a parametric analysis on engine BPR, in order to test the engine surrogate model in an aircraft design and analysis framework. The idea was to use this model to guide the selection of the best suitable engine characteristic in terms of BPR for an advanced narrow-body aircraft, with an expected EIS in 2030. For this purpose, the baseline aircraft was equipped with advanced airframe technologies such as:

- Riblets, applied on the surface of the fuselage, of the wing, and of the horizontal and vertical tails, and allowing to reduce the zero-lift drag coefficient of the airplane.
- Bleed-less MEA architecture, where:
    - External compressors, powered by the electric system, feed the environmental control system (ECS), while the ice protection system (IPS) is totally electrified.
    - The electric system powers the electric pumps of the hydraulic system, which in turn supplies the flight control system (FCS), the actuators for the landing gears, and the wheel brakes.
- Carbon-Fiber-Reinforced Polymers (CFRP) usage for the main structures of the fuselage, of the wings, and of the tails.
- Advanced Ti-based alloys for the main structures of the landing gears system.

In order to include the effects of these technologies in the MDA framework of JPAD, a strategy essentially based on calibration factors and calibration offset was implemented, as already described in Ref. [3]. To recap:

- A -7.5% of skin friction drag for all the airframe components with riblets applied on them.
- A 2% reduction of the On-Board Systems (OBS) mass and a 190% increase in terms of power off-takes, due to the MEA architecture previously described.
- A 20% weight reduction for the wing and for the tail group, as well as a 25% weight reduction of the fuselage structure, due to the usage of CFRP; a 30% reduction in terms of weight of the landing gear system, thanks to Ti-based alloys.

Assumptions related to the level of technology were performed also for the engines. A 2030 EIS was supposed as the input value for the corresponding variable of the surrogate engine model. An OPR value equal to 55 and a T_4 equal to 1850 K were supposed as adequately realistic for the selected time frame. Input in terms of overboard bleed and power off-takes were automatically set, according to the selected MEA architecture.

The parametric analysis involved 6 different BPR values for the engines, ranging from 9 to 14. For each BPR value, a different aircraft was designed and analyzed, aiming for the fulfillment of the same set of TLAR reported in Table 2. For this purpose, the framework depicted in Fig. 6 was elaborated, by means of the Application Programming Interface (API) provided by JPAD and by its calculation modules. First, the baseline aircraft model was equipped with a new couple of turbofan engines, designed through the surrogate model, featuring a specific BPR value and initial thrust requirements for ToC and T/O EoR equal to the ones of the baseline: 26 kN and 94.5 respectively. This updated aircraft model was then analyzed with JPAD, by means of a complete MDA cycle, as the one reported in Fig. 7. A convergence loop was imposed at this level, in order to correctly assess the design weights of the aircraft, standing the mission requirements of Table 2. The results of the performance analysis in terms of Take-Off Field Length (TOFL), Landing Field Length (LFL), initial cruise Mach number, initial cruise altitude, climb rate, and climb speed were then compared with the set of reference TLAR. In case that one or more requirements were not matched, the aircraft was re-designed, by means of a new sizing point selection. The definition of the constraints of the available design space was supported by the much more detailed and reliable output data produced by the aerodynamics and weights modules of JPAD for MDA, rather than rough values taken from statistics. A strategy for maximum wing loading was selected for the automatic re-design process of the aircraft. The new values coming from the sizing in terms of SLS T/O thrust, wing planform area and wing aspect ratio were used to update the performance, the geometry and the weight of the powerplant, as well as the characteristics of the airframe. With regards to the engine thrust, the new value was used to update the input values of the surrogate engine model in terms of ToC and T/O EoR net thrust, by means of constant scale factors, derived from statistical information and from engineering experience, equal to 0.22 and 0.8 respectively. Dealing with the geometry of the airframe, the wing was automatically updated to match the planform area coming from the sizing. The wing aspect ratio was set as a derived variable, in order to match a target value of the wing span equal to 35.8 m, close to the upper limit set for category C aircraft, according to the ICAO Aerodrome Reference Code (ARC). The automatic update of the aircraft geometry also involved several checks in terms of landing gear system feasibility. After the re-design of the wing and of the powerplant system, the strut length and the wheeltrack of the main landing gears were checked and eventually adjusted, in order to fulfill requirements in terms of minimum engine clearance (set to 0.5 m for this specific study), in-wing retraction allowance, and aircraft rotation angle. For example, an engine characterized by a greater BPR and/or a greater SLS T/O thrust required a longer leg of the main landing gear in order to comply with the minimum engine clearance requirement, and eventually a greater wheeltrack too, to leave sufficient room for the retraction of the wheels. All these modifications were later checked, during the MDA of the aircraft, by the JPAD module dedicated to ground stability analysis, in order to eventually detect issues related to an incorrect positioning of the landing gears with respect to the body of the aircraft.

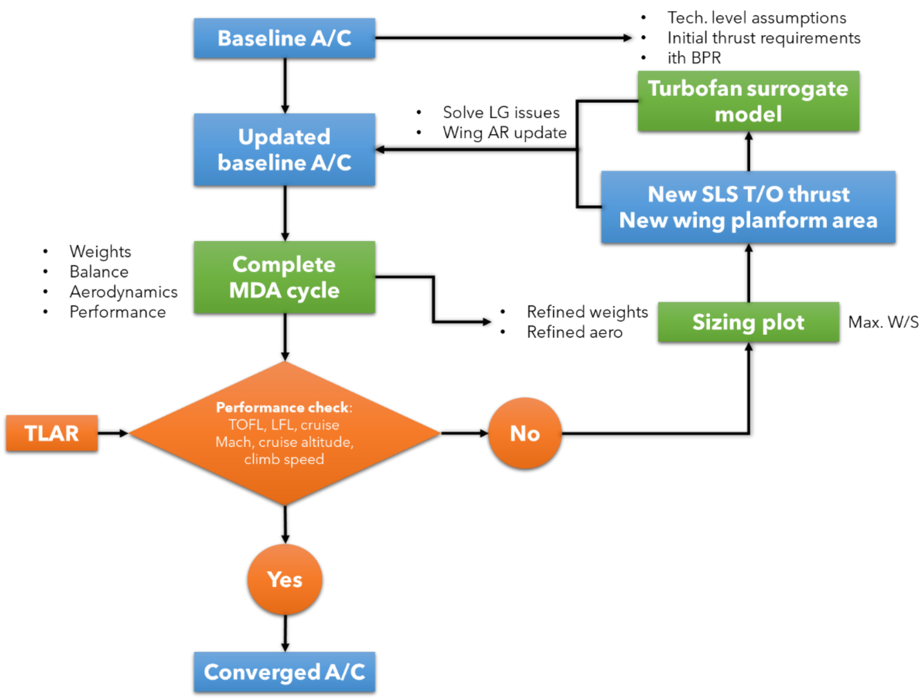

Fig. 6 Aircraft design convergence loop for the parametric study on engine BPR.

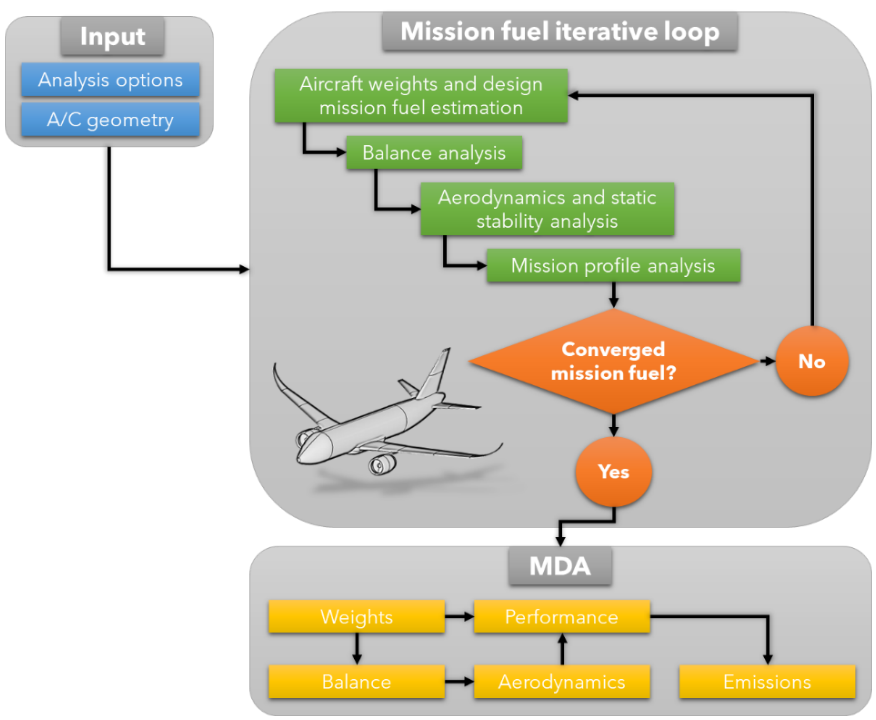

Fig. 7 Aircraft multi-disciplinary analysis cycle, with the convergence loop on mission fuel.

The main results of these analyses in terms of aircraft characteristics and performance have been summarized in Table 4. Table 5, instead, provides the main characteristics of the engines equipped on these aircraft models. The enforcement of the set of TLAR listed in Table 2 led, for each different engine (i.e., for each different BPR value), to a different sizing point in terms of wing loading and thrust-to-weight ratio of the airplanes, as further highlighted in Fig. 8. The increase in weight and size of the engines, due to the growth of the BPR, determined an increment of the OEW of the aircraft, which counteracted the beneficial effect of TSFC decrease on the mission fuel burn and on the MTOW. This latter was also opposed by the increase in nacelle drag, due to the growth of both the nacelle frontal and wetted areas, which led to higher skin friction and form drag. The growth of the nacelle contribution to the total aircraft zero-lift drag has been reported in Fig. 9. Nonetheless, the favorable effect of BPR on TSFC allowed for a decrease in total consumed fuel for the design mission, up to BPR 12. For higher values of this parameter, the total amount of fuel burn and CO_2 emission started to grow, due to the above-mentioned negative effects. All these considerations have been summarized in Fig. 10, which highlights percentage differences in terms of cruise specific fuel consumption, dry mass, maximum nacelle diameter, and nacelle cowl length of the engines automatically designed with the surrogate model, with respect to the BPR 9 engine, here taken as a reference. This same plot also underlines the actual effect at aircraft level of different BPR engines in terms of fuel burn/CO_2 emissions (assuming a constant EI for carbon dioxide) reductions. An up to more than 6% decrease in terms of TSFC did not determine, as expected, an identical reduction of fuel burn, due to the counteraction exerted by the previously mentioned parameters. The plot on the right of the same figure also highlights the well-known “bell curve”, which typically results from similar parametric analyses on engine BPR.

The re-design of the aircraft due to a change in the engine bypass ratio determined a growth of the wing planform surface, in order to make the aircraft compliant with the set of TLAR and with the TOFL and LFL limitations, in particular. In fact, for all the 6 aircraft designed for this study, the sizing point matching the highest possible wing loading was found at the intersection of the T/O and landing constraints. The necessity to fulfill the TOFL requirement also determined an increase of the engine T/O static thrust with the BPR, which brought to a snow-ball effect on the MTOW.

Concerning the landing gears system, automatic adjustment were applied by the JPAD module for geometric issues to all the designed aircraft, in order to meet the above-listed set of requirements. The growth of the nacelles in the transversal dimension determined an increase in the main landing gear leg length, which went from 2.42 m for the BPR 9 engine aircraft, to 2.77 m for the BPR 14 model. For the same reason, also the wheeltrack required to be automatically adjusted, and went from 6.25 m for the lowest BPR engine to 7.13 for BPR 14. It was later checked, during the analysis of each converged aircraft, that these modifications did not negatively impact the ground stability and operability of the aircraft.

Table 4 Main results from the parametric study in terms of characteristics and performance of the 6 different designed aircraft.

	BPR 9 A/C	**BPR 10 A/C**	**BPR 11 A/C**
Wing area, m^2	104.07	105.10	106.05
Wing aspect ratio	12.31	12.19	12.09
MTOW, kg	68826	69247	69721
OEW, kg	38401	38881	39352
W/S, kg/m^2	661.3	658.9	657.4
T/W	0.315	0.317	0.320
Total consumed fuel, kg	15376	15311	15268
Total CO_2 emissions, kg	48419	48240	48248
	BPR 12 A/C	**BPR 13 A/C**	**BPR 14 A/C**
Wing area, m^2	106.80	107.43	107.84
Wing aspect ratio	12.00	11.93	11.88
MTOW, kg	70129	70427	70721
OEW, kg	39764	40054	40322
W/S, kg/m^2	656.6	655.6	655.8
T/W	0.322	0.325	0.327
Total consumed fuel, kg	15250	15265	15307
Total CO_2 emissions, kg	48238	48263	48342

Table 5 Main characteristics of the engines equipped on the set of aircraft of Table 5.

	BPR 9	BPR 10	BPR 11	BPR 12	BPR 13	BPR 14
SFC cruise, g/(kN*s)	14.44	14.21	14.00	13.82	13.68	13.56
Δ% BPR 9	-	-1.64%	-3.07%	-4.30%	-5.32%	-6.14%
SLS T/O thrust, kN	106.29	107.68	109.32	110.72	112.26	113.59
Δ% BPR 9	-	+1.31%	+2.85%	+4.17%	+5.62%	+6.87%
Dry mass, kg	2307	2426	2534	2618	2688	2732
Δ% BPR 9	-	+5.14%	+9.84%	+13.48%	+16.49%	+18.42%
Nacelle max. diameter, m	2.177	2.265	2.353	2.434	2.514	2.588
Δ% BPR 9	-	+4.04%	+8.08%	+11.81%	+15.48%	+18.88%
Nacelle cowl length, m	3.212	3.310	3.406	3.493	3.576	3.652
Δ% BPR 9	-	+3.05%	+6.04%	+8.75%	+11.33%	+13.70%

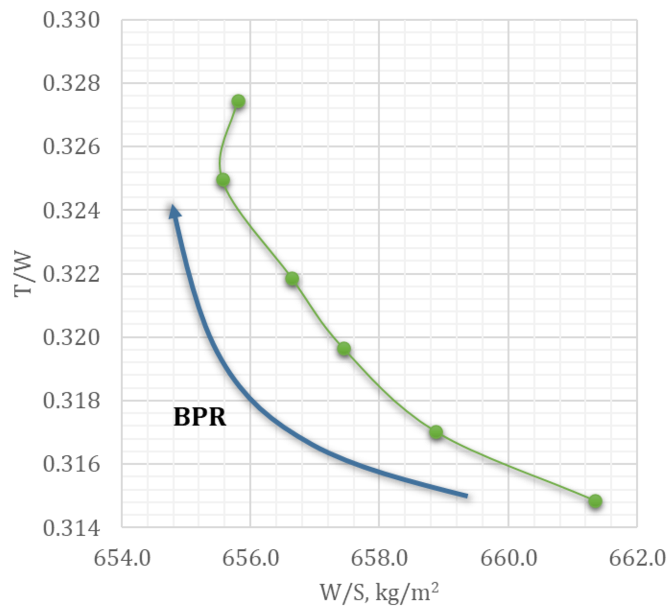

Fig. 8 Aircraft sizing point evolution with respect to changes to the BPR of the engines.

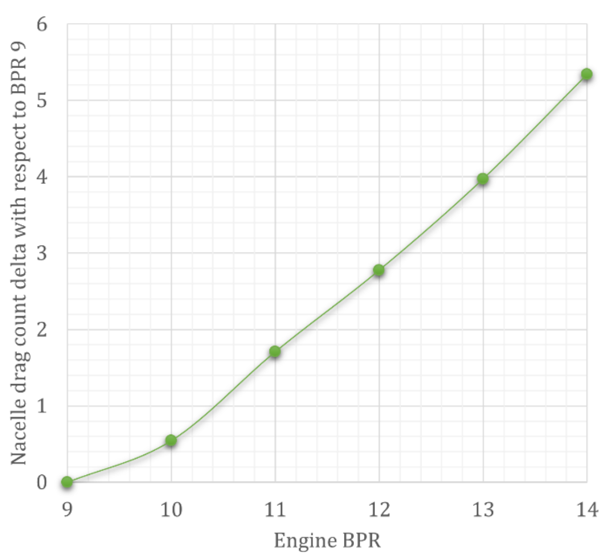

Fig. 9 Growth of the nacelles contribution to the aircraft zero-lift drag with increasing BPR.

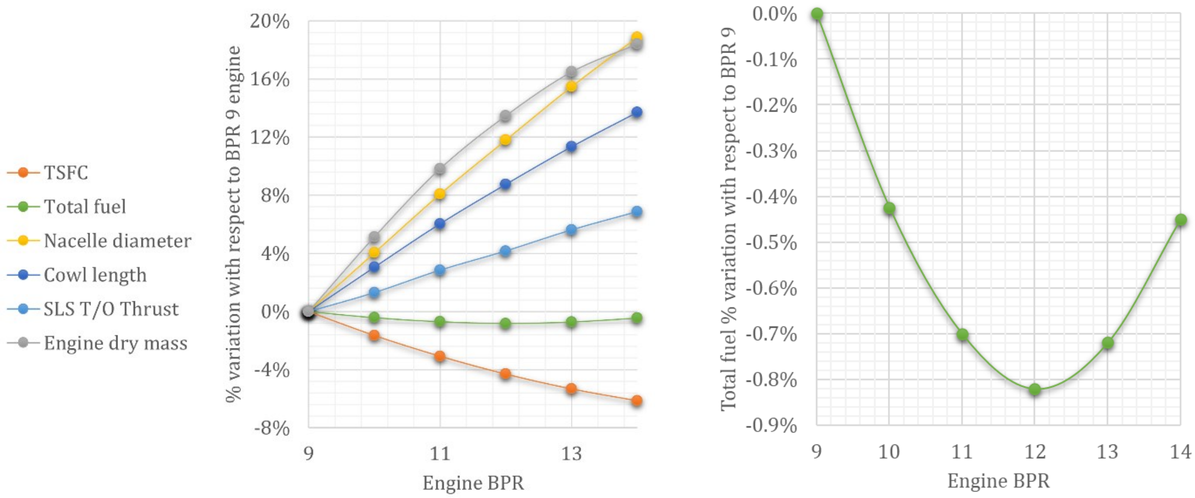

Fig. 10 Percentage changes (with respect to the BPR 9 engine) of the characteristics and performance of the powerplant system, for the 6 aircraft models designed for a different BPR of the engines. The plot on the right provides a close-up on the total fuel consumed by the aircraft for the design mission.

VI. Conclusions

The previous sections have provided an overview on a possible approach for an effective and consistent modeling of gas turbine engines for aeronautical applications, allowing to include the effects of changes to the characteristics of the engine in a typical aircraft preliminary design workflow. In particular, the methodology reported in Section IV applies to the case of a turbofan engine and allows to carry out meaningful preliminary estimations on the specific fuel consumption, dry mass, engine/nacelle size, costs, and environmental noise, starting from rather simple input assumptions on the level of technology, on the bypass ratio, and on the off-takes.

A surrogate model representative of a high bypass ratio, direct-drive, unmixed flow turbofan was implemented in JPAD, an existing tool, in-house developed at UNINA, allowing to carry out civil aircraft preliminary design activities. Then this surrogate model was tested in a parametric study concerning BPR, for the design of an advanced (EIS 2030) short-haul, narrow-body aircraft, including new engines and innovative airframe technologies. This analysis returned physically plausible results, generally in line with expectations. A total fuel burn/CO_2 emissions reduction greater than 20% was predicted with respect to a today's aircraft, which also agrees with the requests coming from the agendas on global warming, further highlighting the potential of JPAD as a standalone tool.

References

[1] http://www.adorno-project.eu/, retrieved online April 30, 2022.

[2] Nicolosi, F., Della Vecchia, P., Trifari, V., Di Stasio, M., Marulo, F., De Marco, A., Marciello, V., and Cusati, V., "Noise, Emissions, and Costs trade factors for regional jet platforms using a new software for aircraft preliminary design", *AIAA Aviation 2020 Forum*, AIAA, Virtual Meeting, 2020, doi: 10.2514/6.2020-2638.

[3] Di Stasio, M., Trifari, V., Nicolosi, F., De Marco, A., Fuhrmann, S., and Schaber, R., "Multidisciplinary Optimization of a Regional Jet Including Advanced Airframe and Engine Technologies", *AIAA Aviation 2021 Forum*, AIAA, Virtual Meeting, 2021, doi: 10.2514/6.2021-2424.

[4] Di Stasio, M., "Efficient Gas Turbine Modeling for Low Emission Aircraft Preliminary Design Workflows", Ph.D. Dissertation, Dept. of Industrial Engineering, University of Naples Federico II, Naples, Italy, 2022.

[5] https://www.gasturb.de/. Retrieved online April 30, 2022.

[6] Seitz, A., "Advanced methods for Propulsion System Integration in Aircraft Conceptual Design", Ph.D. Dissertation, Technical University of Munich, Munich, Germany, 2011.

[7] Kurzke, J, "Fundamental Differences Between Conventional and Geared Turbofans", *2009 ASME Turbo Expo: Power for Land, Sea and Air*, Orlando, Florida, USA, 2009, doi: 10.1115/GT2009-59745.

[8] Grieb, H., *Projektierung von Turboflugtriebwerken*, Birkhäuser, Basel, Switzerland, 2004, doi: 10.1007/978-3-0348-7938-5.

[9] Walsh, P.P., and Fletcher, P., *Gas Turbine Performance*, 2nd edition, Blackwell Science, Bristol, 2004, doi: 10.1002/9780470774533.

[10] Kurzke, J., and Halliwell, I., *Propulsion and Power: An Exploration of Gas Turbine Modeling*, Springer, Cham, Switzerland, 2018, doi: 10.1007/978-3-319-75979-1.

[11] Gauntner, J., “Algorithm for calculating turbine cooling flow and the resulting decrease in turbine efficiency”, NASA Technical Memorandum, Lewis Research Center, Cleveland, Ohio, February 1980. NASA-TM-81453.

[12] Samuelsson, S., Kyprianidis, K.G., and Gronstedt, T., “Consistent Conceptual Design and Performance Modeling of Aero Engines”, *ASME Turbo Expo 2015: Turbine Technical Conference and Exposition,* Montreal Canada, 2015, doi: 10.1115/GT2015-43331

[13] Jenkinson, L.R., Rhodes, D., and Simpkin, P, *Civil Jet Aircraft Design*, Butterworth-Heinemann, Oxford, UK, 1999, doi: 10.2514/4.473500.

[14] Engineering Sciences Data Unit (ESDU), “Prediction of noise generated by fans and compressors in turbojet and turbofan engines”, Item no. 98008, ESDU International plc, London, UK, April 1998.

[15] Kim, H.D, “Design methodologies for aerodynamics, structures, weight and thermodynamic cycles”, MIT, 2013, retrieved online April 30, 2022, from: http://web.mit.edu/drela/OldFiles/Public/N+3/Final_Report_App.pdf.

[16] Mattingly, J.D., Heiser, W.H., and Pratt, D.T., *Aircraft Engine Design*, 2nd edition, AIAA, 2002, ISBN: 1600860168.

[17] Kyprianidis, K.G., “Future Aero Engine Designs: An Evolving Vision”, IntechOpen. 2011, doi: 10.5772/19689.

[18] https://it.mathworks.com/help/stats/regression-learner-app.html, retrieved online April 30, 2022.

[19] Casale, C., Polito, T., Trifari, V., Di Stasio, M., Della Vecchia, P., Nicolosi, F., and Marulo F., “Implementation of a Noise Prediction Software for Civil Aircraft Applications”, *XXV International Congress of the Italian Association of Aeronautics and Astronautics,* AIDAA, Rome, Italy, 2019, doi: 10.5281/zenodo.3943793.

[20] Younossi, O., Arena, M.V., Moore, R.M., Lorell, M., Mason, J., and Graser, J.C., “Military Jet Engine Acquisition: Technology Basics and Cost-Estimating Methodology”, RAND Corporation, 2003, retrieved online April 30, 2022, from: https://www.rand.org/pubs/monograph_reports/MR1596.html.

[21] Torenbeek, E. *Advanced Aircraft Design - Conceptual Design, Analysis and Optimization of Subsonic Civil Airplanes*. John Wiley & Sons, Chichester, UK, 2013.

[22] De Marco, A., Trifari, V., Nicolosi, F., and Ruocco, M, “A Simulation-Based Performance Analysis Tool for Aircraft Design Workflows”, Aerospace, Vol. 7, Issue 11, 2020, doi: 10.3390/aerospace7110155.

Acknowledgments

The project leading to these results (ADORNO) has received funding from the Clean Sky 2 Joint Undertaking under the European Union’s Horizon H2020 research and innovation program under Grant Agreement ENG ITD n° 821043. The authors are grateful to the Topic Leader of the project MTU Aero Engines for its useful feedbacks and suggestions concerning gas turbine engine modeling. The content of this paper reflects only the authors’ view and both the European Commission and the Clean Sky 2 Joint Undertaking are not responsible for any use that may be made of the information it contains. The work reported in this paper does not represent the outcomes of ADORNO, and it is just the result of the collateral collaboration between the partners in the project. The results presented here are the results of UNINA assumptions, and do not include any sensitive information.